第 35 卷第 5 期
2016 年 10 月

红 外 与 毫 米 波 学 报
J. Infrared Millim. Waves

Vol. 35, No. 5
October, 2016

文章编号: 1001 - 9014(2016)05 - 0517 - 04

DOI:10.11972/j.issn.1001 - 9014.2016.05.001

A novel electrode design and implementation for mesa-arrayed infrared detectors

HUANG Yue[1], CHEN Yi-Yu[2], MA Wei-Ping[1], LIU Dan[1], CHEN Yu[1], YE Zhen-Hua[1*], DING Rui-Jun[1], HE Li[1]

(1. Key Laboratory of Infrared Imaging Materials and Detectors, Shanghai Institute of Technical Physics, Chinese Academy of Sciences, Shanghai 200083, China;
2. Graduate School of the Chinese Academy of Sciences, Beijing 100049, China)

Abstract: A novel electrode structure for mesa-arrayed infrared detectors is proposed. A relayed electrode at the bottom of the trench is realized by depositing the electrode twice separately. Comparing with the traditional extended electrode, the novel electrode structure is not only beneficial to simplify the electrode introducing at the bottom of the trench out from the bottom to the top of the trench, but also capable of enlarging the top area on the mesa arrays for other processes and enhancing the structural integration correspondingly. The height and morphology of the relayed electrode were not changed after experiencing 200 W ultrasonic treatment for 5 mins. As shown in the cross-sectional SEM pictures of the flip-chip bonded devices, the relayed electrode at the bottom of the trench connected into a whole and reached the metallization pads on the other side. These results indicated that this new electrode structure can be applied to the mesa-arrayed infrared detectors.

Key words: mesa array, electrode, infrared detector
PACS: 85.60.Dw

一种用于台面探测器的新型电极结构

黄 玥[1], 陈奕宇[2], 马伟平[1], 刘 丹[1], 陈 昱[1], 叶振华[1*], 丁瑞军[1], 何 力[1]

(1. 中国科学院上海技术物理研究所 红外成像材料与器件重点实验室,上海 200083;
2. 中国科学院大学, 北京 100049)

摘要:提出一种用于台面探测器的新型电极结构.该结构通过在台面底部两次制备电极而获得接力电极.同传统的引出电极结构相比,这种接力电极结构不仅简化了从台面底部引出电极的工艺,而且能够增加台面顶部空间从而更有利于其它工艺的进行以及工艺集成.在 200 W 超声处理 5 分钟后,接力电极的高度和形貌都未发生变化.从倒焊互连的剖面 SEM 照片可以看出台面底部的接力电极是个整体,并且该接力电极结构完全可以应用在台面探测器中.

关 键 词:台面;电极;红外探测器

中图分类号:TN303; TN305 **文献标识码**:A

Introduction

There are two materials for detectors that can sense light over an unusually broad range of wavelengths from infrared to microwave radiation. One is graphene[1] and the other is mercury cadmium telluride (HgCdTe) semiconductor. HgCdTe-based photovoltaic detectors offer tunable bandgap[2], fast response times, high sensitivity and operating temperatures[3-4] over other infrared detectors. The second generation of HgCdTe-based infrared detectors has been mature at the production level since 2001[5]. According to the common understanding, the third generation of infrared detector is expected to pro-

Received date: 2015-06-15, **revised date**: 2016-05-08 **收稿日期**:2015-06-15, **修回日期**:2016-05-08
Foundation items:Supported by the national natural science foundation ot China (61404148,61534006)
Biography:Biography: Huang Yue (1983-), female, Henan, Associate professor, PhD. Working on flip-chip bonding technology right now. E-mail: huangyue@mail.sitp.ac.cn
* **Corresponding author**:E-mail: zhye@mail.sitp.ac.cn

vide advanced functionalities like more pixels, multicolor or multiband capability, high frame rates and good thermal resolution[6]. Besides the ion implantation process, there are diffusion process and the mesa structure process to form p-n junction of the HgCdTe-based infrared detectors[7]. For the mesa structure, it is requisite to obtain trenches with high aspect ratio which can effectively isolate the detector pixels[8] as well as introduce the signal at the bottom of the trenches[9]. The signal at the bottom of the trench was traditionally introduced out from the bottom of the trench to the top, the so-called extended electrode (seen in Fig 1). Since the format and performance requirements for the 3rd generation of infrared detector are almost the same as the formers, the reduction of the pixel pitch is necessary.

As the pixel pitch reduced dramatically from Xμm to X/nμm ($n>1$), the extended electrode on the top of the trench will be problematic even the pixel size scaled down in the meantime. The first issue is that the distance between the adjacent electrodes on the top of the trench will be small. This is a huge challenge for mass production as well as for flip-chip bonding. The aspect ratio of the trenches needs to be further enhanced as the opening of the trench might scale down simultaneously leading to nearly vertical sidewalls of the trench. This makes passivation the second question that should be concerned. The reliability of the extended electrode, particularly the part covering the sidewalls of the trench, is the third matter that deserves investigation. Therefore, we illustrate a novel electrode structure for mesa-arrayed infrared detectors. The electrode at the bottom of the trench is introduced directly from the bottom of the trench in this new structure. By depositing the electrode at the bottom of the trench twice, there is a relayed electrode at the bottom of the trench. It is worth to mention that the height and morphology of the relayed electrode at the bottom of the trench barely decreases after 200W ultrasonic treatment for 5mins. The current-voltage (I-V) characteristic of the mesa-arrayed detector using this new electrode structure proves the electrical function of the relayed electrode at the bottom of the trench. And the cross-sectional picture after flip-chip bonding of the mesa-arrayed detector proves that this new electrode structure can be indeed applied to the mesa-arrayed infrared detectors.

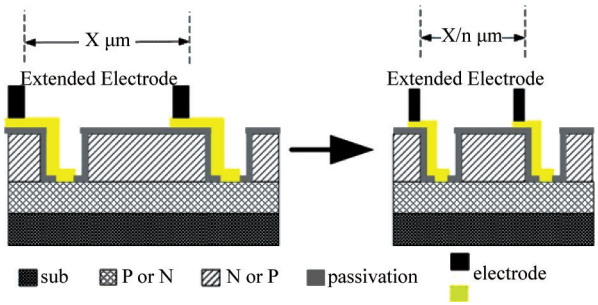

Fig. 1 Schematic diagram of the extended electrode for the mesa-arrayed infrared detector
图1 采用引出电极结构的台面探测器示意图

1 Experiments

The detailed growth procedure of HgCdTe onto GaAs substrate includes the following operation[10]:

-chemical etching of GaAs substrate;

-thermal treatment of GaAs surface in arsenic flux in vacuum;

-growth of CdZnTe buffer layer on an atomic clean GaAs surface;

-growth of HgCdTe on the buffer layer.

The HgCdTe material is cleaned in the sequence of chlorylene, ether, acetone and ethyl alcohol before using. The main fabrication steps include photolithography, formation of trenches, metallization, two separately times of electrode deposition, and flip-chip bonding. The morphology of the relayed electrode at the bottom of the trench was characterized by confocal scanning laser microscope and scanning electron microscopy (SEM). The ultrasonic treatment was used to evaluate the rigidity of the relayed electrode at the bottom of the trench. The I-V measurement was carried out on a cryogenic probe station to testify the electrical function of the relayed electrode at the bottom of the trench.

2 Results and discussions

Figure 2 is the schematic flow chart of the new electrode structure proposed in this article. It can be seen that the top of the relayed electrode at the bottom of the trench is equal to the opening of the trench in the first deposition. Then a relayed electrode at the bottom of the trench is obtained with adjustable height. Comparing with just one deposition of the electrode at the bottom of the trench, it requires less conformality of the photoresist to cover nearly vertical sidewalls of the trench. Also, this two-step deposition solves the dilemma of getting such a tall electrode at the bottom of the trench with high aspect ratio. The most important feature of this new electrode structure is getting rid of metal deposition on the sidewalls of the trench. Comparing with the traditional extended electrode, this will make sure a good reliability of the electrode at the bottom of the trench.

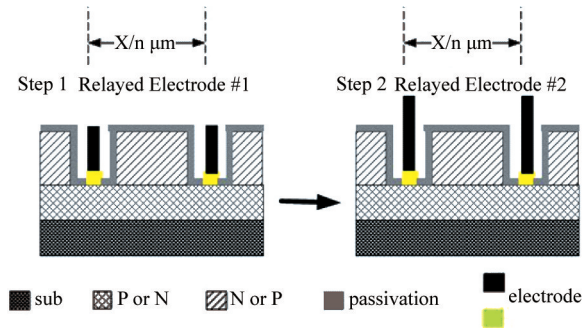

Fig. 2 Schematic flow chart of the new electrode structure for the mesa-arrayed infrared detectors
图2 制备新型台面探测器电极结构的流程示意图

Figure 3 (a) and (b) are the confocal scanning laser profiles of the trenches before and after the deposition of relayed electrode. It is clear that the bottom of the trench is filled after the electrode deposition and the relayed electrode is located in the middle of the bottom of the trench. The cross-sectional SEM picture of the new electrode structure is presented in Fig. 3 (c) in which

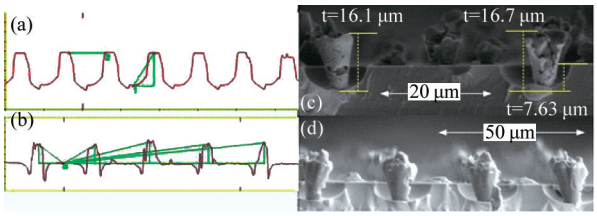

Fig. 3　(a) and (b) are the confocal scanning laser profiles of the trenches before and after electrode deposition; (c) and (d) are the cross-sectional SEM of the new electrode structure before and after ultrasonic treatment

图 3　(a)和(b)分别是制备新型电极前后台面形貌的共聚焦显微镜分析照片; (c)和(d)是新型电极结构在超声处理前后的 SEM 照片

the heights of the two relayed electrodes at the bottom of the trench are 16. 1 μm and 16. 7 μm, respectively. They are indeed in the middle of the bottom of the trench. The heights and morphologies of the relayed electrode at the bottom of the trench barely change after 200W ultrasonic treatment for 5 mins, according to the Fig. 3 (d). It is worth to mention that there is no interface between the two deposition steps regardless of ultrasonic treatment, which is quite different from that of Jiang's results[11]. Jiang and his co-workers have fabricated double-stacked electrodes by electroplating, and there is an obvious interface between the two separated electroplating steps. They did not give any details on the successive electroplating steps, especially the information about the interface. However, the interface could be a potential problem on reliability. Imaging their double-stacked electrode is located at the bottom of the trench, and the protruding of the first-stacked electrode might risk the trench filling with electrode material after flip-chip bonding. Furthermore, they didn't mention the uniformity of the height of the double-stacked electrodes. What's more, their double-stacked electrodes are made on the "dummy wafer" instead of the infrared detectors. Therefore, our relayed electrode at the bottom of the trench is superior to that of Jiang's due to easy deposition, better morphology and uniformity. And our relayed electrode at the bottom of the trench could be treated superficially as a whole. This new electrode structure can be sustainable to smaller pixel size as long as the aspect ratio of the trench keeps.

The typical I-V characteristics of the mesa-arrayed detector using the relayed electrode are shown in Fig. 4. It is clear that both of the two I-V curves are smooth without any abnormal and they are nearly identical. These results testify the electrical function of the relayed electrode at the bottom of the trench. The flip-chip bonding was executed on a FC 150 commercialized device bonder. The pressure was chosen to be two times larger than the usual one in order to testify whether the relayed electrode at the bottom of the trench is a unity or not. The temperature was set to be at room temperature. After flip-chip bonding, the underfill was carried out for the sake of improving the contrast of the SEM picture. Later on, the traditional metallographic specimen preparation is done as in Ref [12]. Figure 5 is the cross-sectional SEM of the flip-chip bonded mesa-arrayed detector using

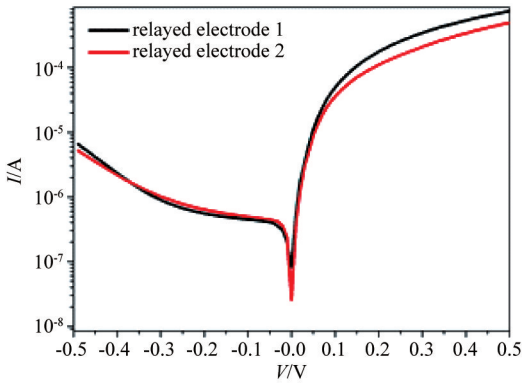

Fig. 4　The typical I-V characteristics of the mesa-arrayed detector using this new electrode structure

图 4　采用新型电极结构的台面探测器的 *I-V* 曲线示意

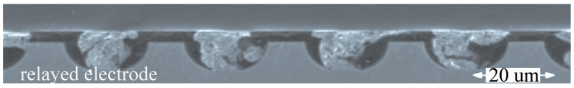

Fig. 5　The cross-sectional SEM of the flip-chip bonded mesa-arrayed detector using the new electrode structure

图 5　采用新型电极结构的台面探测器的互连剖面 SEM 照片

the new electrode structure. It is clear that the size of the relayed electrode decreases from left to right. This is easy to explain since we cannot make sure that the cross-sectional plane of the cutting is right in the middle of all the electrodes. The first scenario might be like that the cross-sectional plane is right in the middle of the first relayed electrode if counting from left, but it exceeds the middle of the rest of the relayed electrodes. And the further it is away from the first relayed electrode, the less its size will be remained. The second scenario could be the opposite that the cross-sectional plane is right in the middle of the fourth relayed electrode but the onset of the first relayed electrode. In this case, most of the electrodes lose during the polishing step of the metallographic specimen preparation. Eventually, only the first electrode shows right in its middle of the cross-sectional plane but others less than half. Despite of various sizes of the remained electrodes, the bonded electrodes are aligned and the trench is not full of the relayed electrodes. Also there is no transverse movement at the interface of the two-step deposited relayed electrodes. Hence, we can conclude that the relayed electrode at the bottom of the trench is essentially a unit. And this new electrode structure can be completely applied to the mesa-arrayed infrared detectors.

3　Conclusion

In order to satisfy the trend of scaling down pixel pitch of infrared detectors as well as overcome the drawbacks of the extended electrode, a new electrode structure for the mesa-arrayed infrared detectors is proposed. The electrode at the bottom of the trench is deposited twice so that its height can exceed the top of the trench

(下转第 633 页)

对机动小目标的自适应检测前跟踪. 相比于 CV-LMB TBD 算法和 IMM-PHD TBD 算法,提出的 IMM-LMB TBD 在保持高精度目标状态估计的同时,具有轨迹级滤波和自适应多模型的优势.

References

[1] Jong A N. IRST and its perspective [C]. Proc. SPIE 2552 on Infrared Technology XXI. San Diego, CA, USA: SPIE, 1995:206 - 213.

[2] Xiong Y, Peng J, Ding M, *et al.* An extended track-before-detect algorithm for infrared target detection [J]. *IEEE Transactions on Aerospace and Electronic Systems*, 1997, **33**(3): 1087 - 1092.

[3] LUO Xiao-xiao. Research on the Technology for High Maneuvering Target Tracking [D]. Changsha: National University of Defense Technology (罗笑冰. 强机动目标跟踪技术研究 [D]. 长沙: 国防科技大学), 2007.

[4] Deng X, Pi Y, Morelande M. Track-before-detect procedures for low pulse repetition frequency surveillance radars [J]. *IET Radar Navigation*, 2011, **5**(1): 65 - 73.

[5] Blackman S S. Multiple hypotheses tracking for multiple target tracking [J]. *IEEE Aerospace and Electronic Systems*, 2004, **18**(1II): 5 - 18.

[6] Chang K, Y B. Joint probabilistic data association for multitarget tracking with possibly unresolved measurements and maneuvers [J]. *IEEE Transactions on Automatic Control*, 1984, AC-**29**(7): 585 - 594.

[7] Mahler R P S. *Statistical Multisource Multitarget Information Fusion* [M]. London, UK: Artech House, 2007.

[8] Maher R. A survey of PHD filter and CPHD filter implementations [C]. Proc. 6567. Orlando: SPIE, 2007:0O - 0O12.

[9] Vo B, Vo B, Pham N, *et al.* Joint Detection and Estimation of Multiple Objects From Image Observations [J]. *IEEE Transactions on Signal Processing*, 2010, **58**(10): 5129 - 5141.

[10] Vo B, Vo B. Labeled random finite sets and multi-object conjugate priors [J]. *IEEE Transactions on Signal Processing*, 2013, **61**(13): 3460 - 3475.

[11] Reuter S, Vo B T, Vo B N, *et al.* The Labeled Multi-Bernoulli Filter [J]. *IEEE Transactions on Signal Processing*, 2014, **62**(12): 3246 - 3260.

[12] Reuter S, Vo B, Vo B, *et al.* Multi-Object Tracking Using Labeled Multi-Bernoulli Random Finite Sets [C]. International Conference on Information Fusion. Salamanca: IEEE, 2014:1 - 8.

[13] Yuan X, Lian F, Han C. Multiple-Model Cardinality Balanced Multitarget Multi-Bernoulli Filter for Tracking Maneuvering Targets [J]. *Journal of Applied Mathematics*, 2013, 2013: 1 - 16.

[14] Tharindu R, Amirali K G, Reza H, *et al.* Labeled Multi-Bernoulli Track-Before-Detect for Multi-Target Tracking in Video [C]. Information Fusion Conference. Washington, DC, USA: 2015:1353 - 1358.

[15] Punithakumar K, Kirubarajan T, Sinha A. A Sequential Monte Carlo Probability Hypothesis Density Algorithm for Multitarget Track-Before-Detect [C]. Signal Data processing small targets. San Diego: SPIE, 2005:1 - 8.

[16] Punithakumar K, Kirubarajan T, Sinha A. Multiple model probability hypothesis density filter for tracking maneuvering targets [J]. *IEEE Transactions On Aerospace And Electronic Systems*, 2008, **44**(1): 87 - 98.

(上接 519 页)

and fulfill the task of introducing the signal. The heights of the two relayed electrodes at the bottom of the trench are 16.1 μm and 16.7 μm, respectively. And their heights and morphologies barely change after 200W ultrasonic treatment for 5mins. The relayed electrode at the bottom of the trench can be regarded as a unity since there is neither noticeable interface nor transverse movement of the two relayed electrodes according to the cross-sectional SEM picture of the flip-chip bonded devices. This means the new electrode structure can be totally applied to the HgCdTe-based mesa-arrayed infrared detectors.

References

[1] SIZOV F, ZABUDSKY V, DVORETSKII S, *et al.* Two-color detector: Mercury-cadmium-telluride as a terahertz and infrared detector [J]. *Applied Physics Letters*, 2015, **106**: 082104.

[2] MELKONIAN L, BANGS J, ELIZONDO L, *et al.* Performance of MWIR and SWIR HgCdTe-based focal plane arrays at high operating temperatures [J]. *Proceedings of SPIE*, 2010: 76602W.

[3] ROGALSKI A, ANTOSZEWSKI J, FARAONE L. Third-generation infrared photodetector arrays [J]. *Journal of Applied Physics*, 2009,**105**: 091101.

[4] PARK BA, MUSCA CA, WESTERHAUT RJ, *et al.* MWIR HgCdTe photodiodes based on high-density plasma-indiuced type conversion [J]. *Semiconductor Science and Technology*, 2008, **23**: 095027.

[5] TRIBOLET P, CHATARD JP, COSTA P, *et al.* MCT technology challenges for mass production [J]. *Journal of Electronic Materials*, 2001, **30**(6): 574.

[6] CABANSKI W, BREITER R, KOCH R, *et al.* 3rd gen focal plane array IR detection modules at AIM [J]. *Proceedings of SPIE*, 2011, **4369**: 547.

[7] TRIBOLET P, CHORIER P, MANISSADJIAN A, *et al.* High performance infrared detectors at Sofradir [J]. *Proceedings of SPIE*, 2000, **4028**: 438.

[8] YIN WT, ZHOW WH, HUANG J. Etch induced damage of HgCdTe caused by inductively coupled plasma etching technique [J]. *Proceedings of SPIE*, 2010: 76584A.

[9] BAVLET JP, ZANATTA JP, CHANCE D, *et al.* Recent Development in Infrared FPAs with Multispectral 128^2 IRCMOS [J]. *Proceedings of SPIE*, 2002, **4650**: 128.

[10] DVORETSKY SA, VARAVIN VS, MIKHAILOV NN, *et al.* MWIR and LWIR detectors based on HgCdTe/CdZnTe/GaAsheterostructures [J]. *Proceedings of SPIE*, **2005**: 59640A.

[11] JIANG JT, TSAO S, O'SULLIVAN T, *et al.* Fabrication of indium bumps for hybrid infrared focal plane array applications [J]. *Infrared Physics & Technology*, 2004, **45**: 143.

[12] HUANG Y, LIN C, YE ZH, *et al.* Reflow flip-chip bonding technology for infrared detectors [J]. *Journal of Micromechanics and Microengineering*, 2015, **25**: 085009.